

AN EFFICIENT ENERGY MANAGEMENT STRATEGY, UNIQUE POWER SPLIT & ENERGY DISTRIBUTION, BASED ON CALCULATED VEHICLE ROAD LOADS

Jeffery B Holtz
AVL Powertrain Engineering
Inc, Plymouth, MI

Faisal J Uppal, PhD
AVL Powertrain Engineering
Inc, Plymouth, MI

ABSTRACT

This paper presents energy management strategy that includes a novel power split and optimization approach for the FED BRAVO program. AVL is responsible for developing and delivering the full hybrid propulsion system integrated into the Fuel Efficient Demonstrator (FED) Bravo vehicle, designed by PRIMUS. The developed energy management algorithm calculates component energy availability, driver demanded torque and manages the distribution of power between propulsion components. This includes a real-time, road load calculated power split between the three propulsion sources, namely Internal Combustion Engine (ICE), Integrated Starter Generator (ISG) and Front Motor (FMOT). Additionally, unique challenges of power split arose between the different propulsion sources due to the particular powertrain architecture selected for this vehicle i.e. a combined through the road and parallel hybrid structure. Specifically, the paper will discuss via case study the road load based power split and optimization methodology employed by AVL Powertrain and implemented on the FED BRAVO.

INTRODUCTION

This paper is a follow-up of [1]. It presents via case study an energy management scheme that includes road load based power split and optimization methodology employed by AVL Powertrain Engineering, Inc. (PEI) for the FED BRAVO vehicle. This represents part of continual effort by AVL using AVL's state of the art simulation and control tools such as CRUISE, DRIVE and AVL HYBRID DESIGN toolkit to design energy efficient vehicles. The main objective of these tools is to help designer strike the right balance between fuel economy, performance, emissions and drive quality (Figure-1). The main goal of the algorithm development for FED Bravo is to improve fuel economy by optimizing the overall hybrid system efficiency while maintaining vehicle drivability and performance.

Content of this paper includes vehicle powertrain architecture, introduction to the road load based efficient power split, energy optimization management scheme and preliminary results.



Figure 1: Vehicle design objectives

FED BRAVO POWERTRAIN ARCHITECTURE

Figure 2 gives an overview of the FED Bravo hybrid system layout and the main powertrain components from a systems viewpoint. There are three propulsion sources in this vehicle: Internal Combustion Engine (ICE), an Integrated Starter Generator (ISG) and the front motor (FMOT). At the rear axle, the engine is coupled to ISG via an electronically

Report Documentation Page

Form Approved
OMB No. 0704-0188

Public reporting burden for the collection of information is estimated to average 1 hour per response, including the time for reviewing instructions, searching existing data sources, gathering and maintaining the data needed, and completing and reviewing the collection of information. Send comments regarding this burden estimate or any other aspect of this collection of information, including suggestions for reducing this burden, to Washington Headquarters Services, Directorate for Information Operations and Reports, 1215 Jefferson Davis Highway, Suite 1204, Arlington VA 22202-4302. Respondents should be aware that notwithstanding any other provision of law, no person shall be subject to a penalty for failing to comply with a collection of information if it does not display a currently valid OMB control number.

1. REPORT DATE 20 AUG 2012	2. REPORT TYPE Journal Article	3. DATES COVERED 20-07-2012 to 19-08-2012	
4. TITLE AND SUBTITLE AN EFFICIENT ENERGY MANAGEMENT STRATEGY, UNIQUE POWER SPLIT & ENERGY DISTRIBUTION, BASED ON CALCULATED VEHICLE ROAD LOADS		5a. CONTRACT NUMBER w56hzv-06-c-0406	
		5b. GRANT NUMBER	
		5c. PROGRAM ELEMENT NUMBER	
6. AUTHOR(S) Jeffery Holtz; Faisal Uppal		5d. PROJECT NUMBER	
		5e. TASK NUMBER	
		5f. WORK UNIT NUMBER	
7. PERFORMING ORGANIZATION NAME(S) AND ADDRESS(ES) AVL Powertrain Engineering,47519 Halyard Dr.,Plymouth,Mi,48170		8. PERFORMING ORGANIZATION REPORT NUMBER ; #23163	
9. SPONSORING/MONITORING AGENCY NAME(S) AND ADDRESS(ES) U.S. Army TARDEC, 6501 East Eleven Mile Rd, Warren, Mi, 48397-5000		10. SPONSOR/MONITOR'S ACRONYM(S) TARDEC	
		11. SPONSOR/MONITOR'S REPORT NUMBER(S) #23163	
12. DISTRIBUTION/AVAILABILITY STATEMENT Approved for public release; distribution unlimited			
13. SUPPLEMENTARY NOTES Submitted to 2012 NDIA GROUND VEHICLE SYSTEMS ENGINEERING AND TECHNOLOGY SYMPOSIUM August 14-16, Michigan			
14. ABSTRACT This paper presents energy management strategy that includes a novel power split and optimization approach for the FED BRAVO program. AVL is responsible for developing and delivering the full hybrid propulsion system integrated into the Fuel Efficient Demonstrator (FED) Bravo vehicle, designed by PRIMUS. The developed energy management algorithm calculates component energy availability, driver demanded torque and manages the distribution of power between propulsion components. This includes a real-time, road load calculated power split between the three propulsion sources, namely Internal Combustion Engine (ICE), Integrated Starter Generator (ISG) and Front Motor (FMOT). Additionally, unique challenges of power split arose between the different propulsion sources due to the particular powertrain architecture selected for this vehicle i.e. a combined through the road and parallel hybrid structure. Specifically, the paper will discuss via case study the road load based power split and optimization methodology employed by AVL Powertrain and implemented on the FED BRAVO.			
15. SUBJECT TERMS			
16. SECURITY CLASSIFICATION OF:			17. LIMITATION OF ABSTRACT
a. REPORT unclassified	b. ABSTRACT unclassified	c. THIS PAGE unclassified	Public Release
			18. NUMBER OF PAGES 12
			19a. NAME OF RESPONSIBLE PERSON

controlled clutch (engine disconnect clutch). ISG is coupled to the rear differential via a six speed fully automatic torque converter based transmission. The differential connects transmission output shaft to the final drives. At the front, there is an electric motor directly coupled to the front differential through a two speed manual gearbox with pneumatic shift actuator. The differential connects to the final drives at the front axle. There are wheel end reduction units (WERU) at front and also at rear connecting to the wheels. The wheels connect the two axles together through the road.

A high power high capacity Li-Ion battery is used to supply power to the electric motors and other HV components and to store the regenerated energy from the electric motors while regenerative braking or simulated engine braking. AVL Hybrid Control System (HCU) coordinates and controls all system components as laid out in Figure-2. HCU is responsible for the power split and energy management functions.

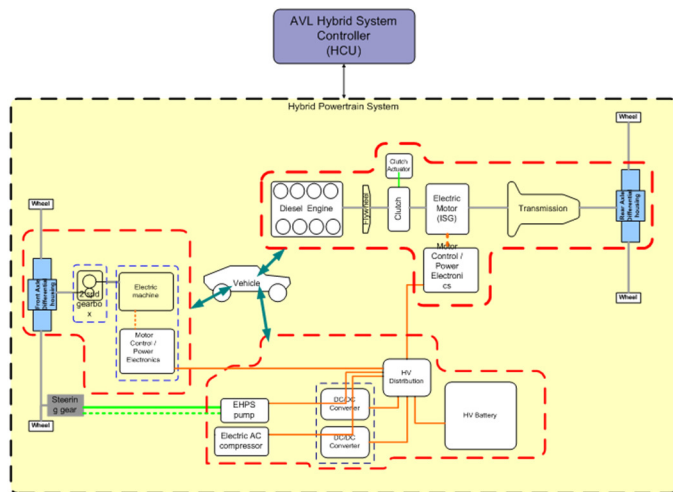


Figure 2: FED BRAVO Hybrid System Layout

CONTROL STRATEGY OVERVIEW

ICE and ISG constitute a parallel hybrid system whereas the inclusion of the FMOT adds Through-The-Road (TTR) hybrid functionality. The main task of the energy management and control design is to utilize all three propulsion sources in the most fuel efficient manner while ensuring minimal performance characteristics.

Figure-3 gives a high level overview of main control tasks in the vehicle. These tasks consist of signal conditioning and powertrain management functions including driver demand calculation, torque management, safety limit monitoring and fault tolerance, component/local and system/global efficiency calculations, power split based on energy management and real-time optimization.

The three main user selectable modes of powertrain operation are 1) Engine only, 2) EV only and 3) Hybrid. There is a great emphasis of smooth transitions between these different modes under varying driving conditions.

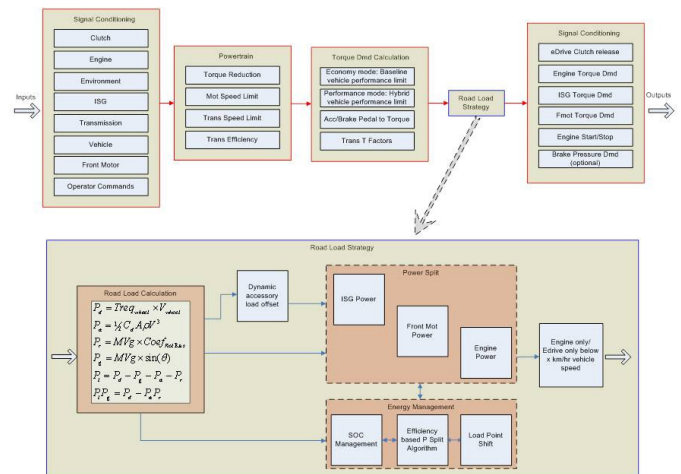


Figure 3: Control Strategy Overview

For real-time computations and management tasks HCU uses pre-determined component characteristic and efficiency maps. Rigorous dynamometer testing has been performed to characterize main hybrid components. The data gathered from the dynamometer testing was used to further fine tune and improve vehicle simulation and control software. Samples of the types of characterization data needed for different powertrain components include; efficiencies, full load curves, thermal characteristics, fuel maps, and shift maps. These key characteristics are confirmed during the dynamometer testing phases and fed back into the base simulation to adjust control parameters and strategy. These modifications further helped steer performance and fuel economy improvements.

In the following sections we will describe the three main components of the control strategy as shown in Figure 3. First we will summarize the Torque Demand Calculation, second the Road Load based Power Split Strategy and then third, the Powertrain/Energy Management Functions.

TORQUE DEMAND CALCULATION AND PERFORMANCE/ECONOMY MODE

Depending on performance or economy mode selection by the user, two separate methods are used for the torque demand calculation. First one is Full load based torque demand $T_{dem_FullLoad}$ and the second one is Road load based torque demand $T_{dem_RoadLoad}$. While the performance mode allows the vehicle to achieve maximum power by the physical hardware components, the economy mode limits the power at the wheels to the plausible power output of the existing HMMWV for the current given inputs based on the current vehicle speed, acceleration pedal, and brake pedal. From this driver requested power at the wheels, the power needed by the hybrid power pack is translated from the wheels through the driveline components, taking the physical components current efficiencies into consideration.

$T_{dem_FullLoad}$ is based on full performance capability of the vehicle and can be described as:

$$T_{dem_FullLoad} = \begin{cases} (T_{min_eng} + T_{min_isg} + T_{min_fmot}) Acc_{ped, pos}, Br_{ped, pos} < \mu_b \\ (T_{max_eng} + T_{max_isg} + T_{max_fmot}) Br_{ped, pos} - T_{min_eng}, Br_{ped, pos} \geq \mu_b \end{cases} \quad (1)$$

$T_{dem_RoadLoad}$ is essentially based on the reference vehicle's (HMMWV in this case) max torque taking into account a) Torque characteristics of the base 6.5L HMMWV engine, b) base HMMWV gear ratios of the 4 speed transmission, c) acceleration and brake pedal pressed for the hybrid vehicle and d) Torque converter's pump and turbine characteristics for both locked/unlocked modes for the base vehicle.

The trade-off between fuel economy and performance is tightly coupled. The main objective of the FED program is to demonstrate the fuel economy savings potential by utilizing the selected hybrid powertrain architecture. This means that there was little benefit in outperforming the baseline vehicle according to the mission profile. To not exceed the baseline vehicles capability, while also maintaining the potential to exhibit the full performance characteristics of the powertrain, a powertrain mode switch can enable different operating conditions.

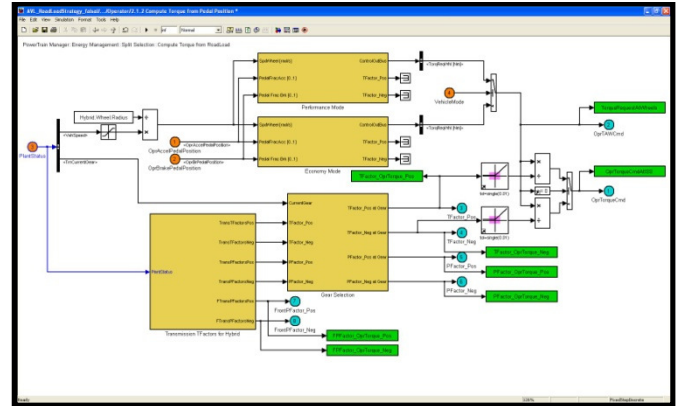


Figure 4: Torque demand calculation

ROAD LOAD BASED POWER SPLIT STRATEGY

Developed by AVL NA, 'AVL Road Load Based Power Split for HEV' is a novel approach based on vehicle road loads that can be used to split the power demand between propulsion sources in a hybrid electric vehicle.

Essentially, the main idea behind the approach is that slow varying or dynamically more stable loads are supported by the engine which generally exhibits higher efficiency at these stable load conditions, whereas rapidly varying or transient loads are supported by the electric motors which are capable of higher efficiencies at these varying loads.

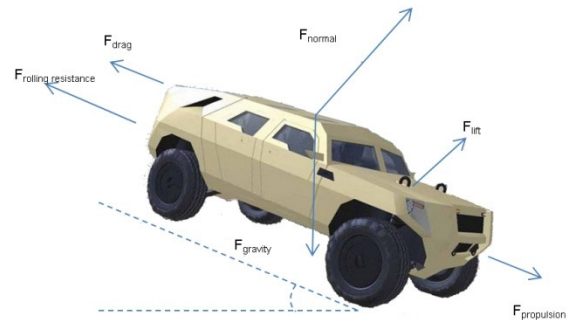


Figure 5: Forces acting on vehicle

Let us examine the forces acting on a vehicle. As shown in Figure 5, six of these main forces are [2, 3]:

1) Rolling Resistance: F_r is a resistance force due to tire deformation in contact with the road surface:

$$F_r = C_{r1}v + C_{r2}F_N \quad (2)$$

C_{r1} and C_{r2} can be experimentally estimated and is usually provided by the tire manufacture.

2) Aerodynamic Drag: This is caused by the loss of momentum of air particles as air flows over the vehicle and depends on the vehicle frontal area, shape, vehicle speed and air density.

$$F_a = \frac{1}{2}v^2 A_f C_d \rho \quad (3)$$

3) Aerodynamic Lift: Similar to the aircraft the aerodynamic lift is a force caused by different pressures between the top and bottom of the vehicle due to different air paths.

$$F_l = \frac{1}{2}v^2 A_l C_l \rho \quad (4)$$

where A_l is the area affecting the lift.

4) Gravitational force: The gravitational force can be decomposed into two components. First one is normal to the road surface and second is in the dimension of vehicle travel. The component of gravitational force in the dimension of vehicle movement is calculated from trigonometric relations as:

$$F_{g1} = \sin\{\alpha\} mg \quad \text{and} \quad \alpha = \tan^{-1}(G) = \tan^{-1}\left(\frac{c}{d}\right) \quad (5)$$

$$F_{g1} = \sin\left\{\tan^{-1}\left(\frac{c}{d}\right)\right\} mg$$

5) Normal force: The normal force is the force exerted by the road on the vehicle's tires the magnitude of which is equal to that of the gravitational force normal to the road.

$$F_N = F_{g2} - F_l = \cos\left\{\tan^{-1}\left(\frac{c}{d}\right)\right\} mg - \frac{1}{2}v^2 A_l C_l \rho \quad (6)$$

6) Propulsion force:

$$F_p = F_{isg_w} + F_{fmot_w} + F_{eng_w} \quad (7)$$

where F_{isg_w} , F_{fmot_w} and F_{eng_w} are ISG, FMOT and ENG equivalent propulsion forces at the wheels.

Power Split Strategy

Considering the total power demand for the vehicle to achieve a target speed v_t and ignoring the aerodynamic lift,

$$P_d = P_i + P_g + P_a + P_r \quad (8)$$

$$P_i = Fv l_d = mav l_d = mv l_d \frac{dv}{dt} \quad (9)$$

$$P_g = \sin(\alpha) mgv l_d \quad (10)$$

$$P_a = \frac{1}{2}v^3 A_f C_d \rho l_d \quad (11)$$

$$P_r = mgv C_r l_d \quad (12)$$

$$\begin{aligned} P_d &= mav l_d + \sin(\alpha) mgv l_d + \frac{1}{2}v^3 A_f C_d \rho l_d + mgv C_r l_d \\ &= v l_d \left(m \frac{dv}{dt} + \sin\{\alpha\} mg + \frac{1}{2}v^2 A_f C_d \rho + mg C_r \right) \quad (13) \end{aligned}$$

$$P_d = T_{Dem} \omega_{wheels} \quad (14)$$

where

P_d : Total computed power demand for the vehicle to overcome resistive forces and in order to maintain or achieve the target speed v_t .

P_i : Power required to overcome inertia in order to achieve target speed (W).

P_g : Power required to overcome gravitational forces due to grade changes (W).

P_a : Power required to overcome air drag force (W).

P_r : Power required to overcome rolling resistance (W).

T_{Dem} : Calculated torque demand (Nm).

ω_{wheels} : Wheel speed (Rad/sec).

m : Equivalent mass of the vehicle

g : Standard gravity, $g = 9.81 \text{m/s}^2$

F : Force required by the vehicle mass m , for acceleration a in order to achieve target speed (N).

v : Current vehicle velocity (m/s).

l_d : Vehicle driveline loss factor

G : Road grade, $G=c/d$, c : vertical distance and d : horizontal distance, α is the angle related to G .

A_f : Vehicle equivalent frontal area (m) for drag computation.

C_d : Vehicle drag coefficient.

C_r : Vehicle rolling resistance coefficient or vehicle road coefficient.

μ_b : Threshold for detecting brake pedal pressed

$$\alpha = \tan^{-1}(G) = \tan^{-1}\left(\frac{c}{d}\right)$$

ρ : Air mass density, $\rho = m_a/V_a$ where m_a is mass of air within test volume V_a . At 20°C and at 101kPa, the density of air is approximately 1.2041 kg/m³.

It is interesting to note that the grade sensor is not needed for the engine and motor power split as P_i+P_g can be computed as:

$$P_i+P_g = P_d - (P_a+P_r) \quad (15)$$

As mentioned earlier, in an attempt to minimize engine load variations or load transients, rapidly varying loads such as P_i and P_g are demanded from the electric motors whereas relatively slow varying loads such as P_a and P_r and demanded from the engine:

$$P_{mot} = \left| \left| P_i + P_g \right|_{L_{m-}}^{L_{m+}} \right|_{L_{b-}}^{L_{b+}} \quad (16)$$

$$P_{isg} = |P_{mot} - P_{acclload}|_{L_{isg-}}^{L_{isg+}} \quad (17)$$

$$P_{fmot} = \left| P_{mot} - P_{isg} + |P_{acclload}|_{L_{isg-}}^{L_{isg+}} \right|_{L_{fmot-}}^{L_{fmot+}} \quad (18)$$

$$P_{eng} = P_a + P_r + \left\{ \{P_i + P_g\} - \{P_{isg} + P_{fmot}\} \right\} \quad (19)$$

where $\{P_i + P_g\} - P_{mot}$ is remaining part of $P_i + P_g$ (P_{mot} overflow) that the motors could not support because of either motor torque/current/temperature limits or battery current/temperature/SOC limits.

L_{m+} , L_{m-} are combined motors' positive and negative limits peak or continuous.

L_{b+} , L_{b-} are battery positive and negative limits peak or continuous.

Objective Function for Optimization for an efficiency based motor power split

For the optimization task, an objective function is formed that reflects the overall potential power losses from the main powertrain components. This constitutes a minimization problem that requires evaluation over several iterations.

Let us construct an objective function Ψ_t that represents all main power losses in the powertrain system from minimization point of view.

$\Psi = f(\chi)$, $\chi = [0, 1/\eta, 2/\eta, \dots, \eta/\eta]$, $\eta =$ number of equally spaced points that define the power split between ISG and FMOT. $\chi = 0$ corresponds to all of the motor power demand P_{mot} assigned to ISG and $\chi = 1$ corresponds to all motor power demand assigned to FMOT.

$$P_{isg} = \{P_{mot} \times [0, 1/\eta, 2/\eta, \dots, \eta/\eta]\} - P_{acclload} \quad (20)$$

$$P_{fmot} = \{P_{mot} \times [\eta/\eta, \dots, 2/\eta, 1/\eta, 0]\} \quad (21)$$

$$P_{eng} = P_d - [P_{isg} + P_{fmot}] \quad (22)$$

$$\Psi_t = |\Psi_{fmot}| + |\Psi_{isg}| + |\Psi_{eng}| + |\Psi_{fgbox}| + |\Psi_{rgbox}| \quad (23)$$

where $P_{acclload}$ represents total high voltage load at the HV battery including export power, DCDC, HV hydraulic pump, HV air conditioning unit etc. Ψ_{fmot} , Ψ_{isg} , Ψ_{eng} , Ψ_{fgbox} and Ψ_{rgbox} are losses associated with the front motor, ISG, Engine, front gearbox and rear gearbox respectively and are calculated based on pre-determined efficiency maps stored in controller memory.

Minimizing Ψ_t wrt χ yields:

$$\begin{aligned} \chi_{opt} &= \arg \min_{\chi \in [0, 1/\eta, 2/\eta, \dots, 1], \eta \in \mathbb{I}} \{\Psi_t(\chi)\} \\ &= \arg \min_{\chi \in [0, 1/\eta, 2/\eta, \dots, 1], \eta \in \mathbb{I}} \left\{ |\Psi_{fmot}| + |\Psi_{isg}| + |\Psi_{eng}| + |\Psi_{fgbox}| \right. \\ &\quad \left. + |\Psi_{rgbox}| \right\} \end{aligned} \quad (24)$$

Such that

$$\begin{aligned} \|\chi - \chi_{opt}\| &\leq \delta \text{ for } \delta > 0 \\ \Psi_t(\chi_{opt}) &\leq \Psi_t(\chi) \end{aligned} \quad (25)$$

holds true i.e on some region around χ_{opt} all of the function values Ψ_t are greater than or equal to the value at that point, (from standard form of an optimization problem) [5].

Note that χ_{opt} may be a local or global minimum depending on the objective function surface and the optimization algorithm used.

There are a large number of algorithms available for solving non-convex problems with some methods that are more complex but are better at finding global minimum than getting stuck at a local one. There are derivative based or search based methods.

In this application, for computational convenience and for dealing with possible discontinuity, the Nelder-Mead Simplex Method (Walsh, 1975) was used. Algorithm was initialized with a grid of uniformly spaced values. Nelder-Mead Simplex is an unconstrained non-linear optimization method. It is a non-gradient based direct search method which is generally less efficient for problems of higher orders but is more robust for problems which are highly discontinuous. It can be used to solve non-differentiable problems. However, this method may only give local solutions so it is important to start with a good initial estimation or a fine grid.

In order to avoid unnecessary switching between Front Motor and ISG or to avoid rapid changes or oscillations on the torque demands, a hysteresis loop is formed around power split changes. Calibrated threshold values are used for a minimum objective function change for the power shift to take place either from front to rear or from rear to front.

For implementing such an optimization in real time it is important to stay well within the limits of processing requirements for the hardware target, while maintaining acceptable algorithm accuracy. That essentially means that in order to minimize the computational effort, a careful compromise is required between the number of iterations and the minimization goal.

POWERTRAIN MANAGEMENT/ ENERGY OPTIMIZATION MANAGEMENT SCHEME

Important functions of powertrain management/energy management optimization include SOC management, power split method selection, HV Accessory load offset, powertrain component safety limit management, powertrain mode management that decides when to allow any user demanded powertrain mode, manage idle speed regulation, compute torque and power factors, store and maintain component characteristics including efficiency tables and full load curves. Some of these functions are described in more detail in the following.

SOC Management

One of the main functions of energy management component is controlling the high voltage battery state-of-charge (SOC). SOC management aims to maximize vehicle fuel economy while maintaining SOC within safe and acceptable limits. Also, in order to maximize battery life and usable capacity for propulsion and regeneration, it is generally desirable to operate it within tightly controlled bounds around the mid-range. However, in order to obtain a

long EV range a high initial SOC is required. In determining the compromise between these two objectives, a number of drive cycles were selected specifically for this vehicle's desired application and used during the simulations for determining this tradeoff.

To deal with this, SOC management upper and lower variable bounds are defined within which the battery SOC is maintained. While always allowing maximum possible regeneration, the e-motor propulsion power limit is varied relative to the maximum and minimum allowable SOC bounds.

This is achieved by defining a motor maximum power coefficient.

$$0 \leq C_{MotMaxPower} \leq 1 \quad (26)$$

This motor maximum power coefficient $C_{MotMaxPower}$ is dependent on the SOC manager State and Battery SOC.

One exception to this is during e-Motor launch assist, when vehicle is starting to move from a stand-still and high acceleration is demanded characterized by acceleration pedal position > 95% and transmission in low gear. In this case $C_{MotMaxPower} = 1$, otherwise it depends on the SOC manager State.

Two SOC States are defined and use different upper and lower limits for the motor maximum power factor:

1. Charge Depletion State. In this state, higher power is allowed for propulsion and as a result more battery power is utilized. This state is characterized by:

$$SOC_{Min_CD} \leq SOC \leq SO_{Max_CD} \quad (27)$$

It is based on above defined minimum and maximum SOC thresholds and in this state motor maximum power factor is computed between thresholds $MotMaxP_{LoLim_CD}$ and $MotMaxP_{HiLim_CD}$.

2. Charge Acquisition State. In this state less motor propulsion power is allowed so that battery can acquire and store charge from regeneration. This is characterized by:

$$SOC_{Min_CA} \leq SOC \leq SOC_{Max_CA} \quad (27)$$

In this state motor maximum power factor is computed between thresholds $MotMaxP_{LoLim_CA}$ and $MotMaxP_{HiLim_CA}$.

Depending on the SOC state, $C_{MotMaxPower}$ is calculated as:

$$C_{MotMaxPower} = SOC_{norm} \times (MotMaxP_{HiLim} - MotMaxP_{LoLim}) + MotMaxP_{LoLim} \quad (28)$$

$$SOC_{Lim} = |SOC|_{SOC_{min}}^{SOC_{max}} \quad (29)$$

$$SOC_{norm} = \left(\frac{SOC_{Lim} - SOC_{Min}}{SOC_{Max} - SOC_{Min}} \right) \quad (30)$$

where SOC_{min} , SOC_{max} , $MotMaxP_{LoLim}$ and $MotMaxP_{HiLim}$ are dependent on SOC State i.e Charge Depletion or Charge Acquisition, SOC_{norm} is normalized state of charge between the limits and SOC_{Lim} is SOC value saturated between the SOC limits.

Figures 6 and 7 show how this management scheme may be performed with examples at two different SOC operating points. At higher battery SOC the demanded e-motor propulsion power is delivered without applying any upper limits, as shown in Figure 6. When the battery SOC becomes low the e-motor provides maximum regeneration but is limited in maximum propulsion power, as can be seen from Figure 7. This allows the battery to absorb all potential energy savings and cap the maximum propulsion to the sum of the absorbed energy.

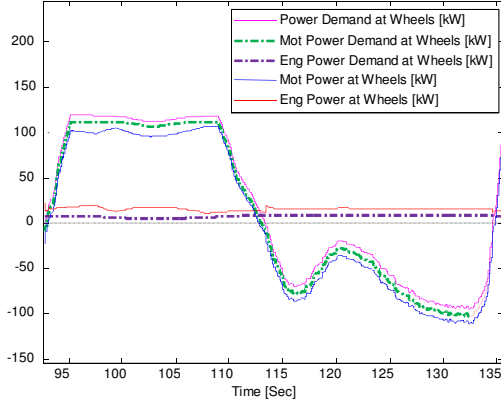


Figure 6: No eMotor power limits in effect at higher battery SOC

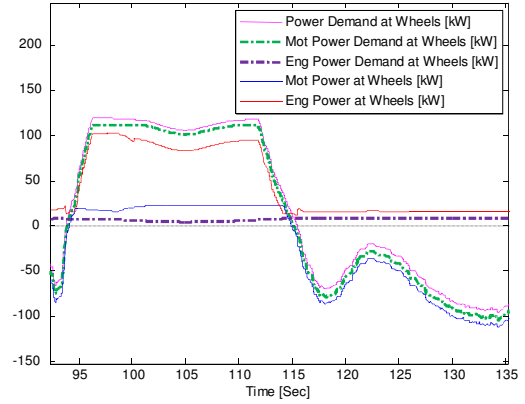


Figure 7: eMotor power limit in effect at lower battery SOC

Simple, Efficiency based and 4x4 based power split

In this application, three methods of power split were used depending on the user selectable controls.

For a simple power split, first the power demand was split between the engine and motors based on the road load equations [16,17,18 & 19]. P_{mot} is first demanded from the ISG and then due to ISG limits the remaining power is demanded from FMOT.

For efficiency based split, the division between engine and the motors was the same as the simple split but further division between the motors: ISG and FMOT is based on an efficiency based optimization algorithm, described by equations [20, 21 and 22].

The third power split method, called the 4x4 power split was developed for off-road situations where a 70:30 split was applied between rear and front axle and then 50:50 split between engine and ISG. This can be described as:

$$P_{fmot} = \left| \left| \frac{3}{10} P_d \right|_{L_{fm-}}^{L_{fm+}} \right|_{L_{b-}}^{L_{b+}} \quad (31)$$

$$P_{isg} = \left| \left| \frac{7}{20} P_d - P_{accload} \right|_{L_{isg-}}^{L_{isg+}} \right|_{L_{b-}}^{L_{b+}} \quad (32)$$

$$P_{eng} = \frac{7}{20} P_d + \left\{ \frac{7}{20} P_d - P_{isg} \right\} + \left\{ \frac{3}{10} P_d - P_{fmot} \right\} \quad (33)$$

$$= \frac{7}{10} P_d - P_{isg} + \frac{3}{10} P_d - P_{fmot}$$

$L_{m+/-}$, $L_{isg+/-}$ and $L_{b+/-}$ are dynamic positive and negative limits of the motors and HV battery depending on speed, temperature and battery SOC.

HV Accessory Load Offset

Accessory load offset is the amount of power demand that is offset from ISG to engine in order to take into account all the accessory related electrical loads of the HV battery.

This is computed taking into account a history of both high voltage load P_{HVLoad} and load offset $P_{AccLoadOffset}$, projected motor and battery efficiencies, battery capacity and motor limits and a vehicle velocity dependent scaling factor μ as follows.

$$\text{Let } P_1(k) = P_{HVLoad}(k) \quad (34)$$

If $P_5(k)$ is the electrical power demanded from ISG to compensate for the accessory loads (Equation 38), an estimate of error can be computed as:

$$P_2(k) = \frac{(P_1(k-1) - P_5(k-1))}{100} \text{ (previous error estimate)} \quad (35)$$

This error term is integrated taking battery efficiency into account in order to get an accumulated error term:

$$P_3(k) = P_2(k) \times \eta_{bat} + P_3(k-1) \text{ where } P_3(0) = 0 \quad (36)$$

Applying accessory load limit ($Lim_{isg}-P_1$), ISG and battery limits yields $P_4(k)$:

$$P_4(k) = \left| \left| P_1(k) + |P_3(k)| \right|_{(Lim_{isg}-P_1)}^0 \right|_{Lim_{isg}-}^{Lim_{isg}+} \left| \right|_{Lim_{Bat-}}^{Lim_{Bat}+} \quad (37)$$

A scaling factor $\mu_{velocity}$ is used to reduce or disable accessory load offset at low speeds for drivability and performance considerations.

$$P_5(k) = \mu_{velocity} \times P_4(k) \quad (38)$$

$P_5(k)$ is rate limited by a factor to avoid sudden changes in demanded power from ISG.

$$P_5(k+1) = \Delta t \times \gamma_{RateLim} \times P_5(k) \quad (39)$$

The final mechanical accessory load offset $P_{AccLoadOffset}(k)$ is computed by multiplying $P_5(k)$, which is essentially the electrical load offset, by ISG efficiency as:

$$P_{AccLoadOffset}(k) = \eta_{isg} \times P_5(k) \quad (40)$$

Hybrid Controller Powertrain Manager (HCPM)

For reasons of safety, performance and energy availability, the vehicle level powertrain management determines whether or not a) to allow Engine Only, EV only and Hybrid powertrain modes, b) to allow 4x4 propulsion mode and c) to allow performance mode.

Safety limit management includes maximum and minimum peak and continuous motor, engine, transmission, front gearbox torque and speed limits at current operating conditions, vehicle speed based limits, special limits in case of component warnings and component heat ups, limits for special maneuvers like step climb and 60% grade.

HCPM also manages system idle speed regulation in different powertrain propulsion modes. The transmission requires a minimum input shaft speed in order to generate pressure for its operation. Idle speed is regulated by ISG, Engine or both depending on the propulsion mode. In 'EV Only' mode it is regulated by ISG as the engine disconnect clutch is disengaged. In 'Engine Only' mode the engine is used to regulate idle speed and in 'Hybrid' mode, both engine and ISG are responsible for regulating idle speed. Special care has to be taken for ISG regeneration torque control near idle speed in order to avoid dipping below idle speed and stalling the motor. Smooth and controlled reduction in ISG regeneration torque close to idle speed is required otherwise torque oscillations or instability can occur.

HCPM computes Torque factors and Power factors based on transmission, differential and gear reduction ratios and efficiencies.

It stores and can also maintain efficiency tables for Transmission, Front Motor, ISG and Engine. It can compare the current component efficiency to that of pre-determined maps and report any inconsistencies. This information can be very helpful in diagnosing faults and issues in these components.

PRELIMINARY SIMULATION/DYNO/VEHICLE RESULTS

This section compares the simulation results for a number of simulation runs with the actual vehicle data. Three types of drive cycles are used for this comparison called the Primary Roads (highways), Secondary Roads (off road low grades) and Trails (off road higher grades).

The first two sets of results are hybrid vehicle in engine only mode. The last three sets are for the hybrid vehicle in full hybrid mode with three different configurations. The table gives percentage values for the mpg improvement over baseline/conventional vehicle simulation and over hybrid vehicle engine only simulation where applicable. Figure 8 provides a graphical representation of comparison for different simulation runs.

Model/Vehicle	% Improvement over conventional Simulation			% Improvement over Hyb veh eng only elect loads sim		
	Primary	Trails	Secondary	Primary	Trails	Secondary
Hybrid veh - Elec loads	63%	38%	32%	x	x	x
Hybrid veh - Mech loads	72%	42%	46%	x	x	x
Hybrid veh - Full Motor	55%	29%	23%	-5%	-6%	-7%
Hybrid veh - Motor Limit	82%	61%	37%	12%	17%	4%
Hybrid veh - Eff Alg	92%	76%	41%	18%	28%	7%

Table 1: Simulation runs - fuel consumption summary

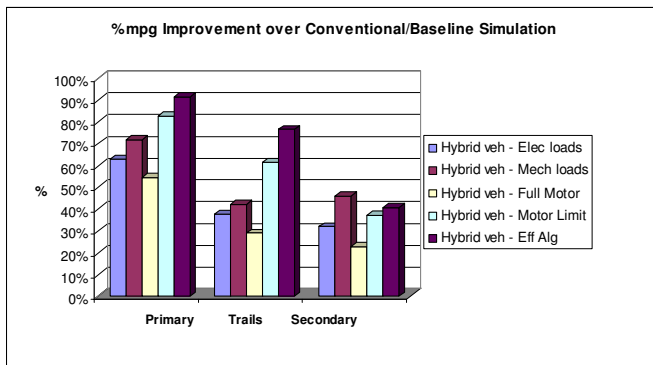


Figure 8: % mpg comparison of simulations runs

The last three simulation runs are described below in more detail:

Hybrid vehicle with simple power split - full motor mode

In this simulation run, full motor limit of 195 kW was used for all three drive cycles i.e. Primary, Trails and Secondary. The initial SOC was selected as 90% for all the simulation runs. Electrical accessory loads were simulated as 5.5kW. Brakes were simulated as a combination of regenerative and friction brakes with a 34% dead-band on the brake pedal.

Table 2 gives a summary and comparison of simulation results in terms of kg of fuel utilized. For Primary roads for example fuel efficiency increase of 36.7% and 35.3% was seen w.r.t the actual and baseline vehicle simulation whereas a decrease of fuel efficiency -5.2% was observed w.r.t hybrid vehicle engine only mode as a result of using full motor propulsion power without SOC management as was expected.

Sim	Model/Vehicle	Primary Roads	Trails	Secondary Roads
		Diff wrt actual (7711kg), baseline and eng only(%)	Diff wrt actual (7711kg), baseline and eng only(%)	Diff wrt actual (7711kg), baseline and eng only(%)
3	Hybrid veh with Simple power split - full motor HEV mode with full motor propulsion power, dynamic acc load offset.	36.7% 35.3% -5.2%	24.0% 22.5% -6.8%	13.8% 18.6% -7.4%

Table 2: Simulation results for Hybrid vehicle with simple power split - full motor mode.

Figure 9 is a graphical representation of the road load power components (P_i+P_g and P_a+P_r) and power split between the engine (P_{eng}) and the motors (P_{mot}). It can be seen that the engine load is maintained around P_a+P_r which is far less varying than the P_i+P_g provided by the motors.

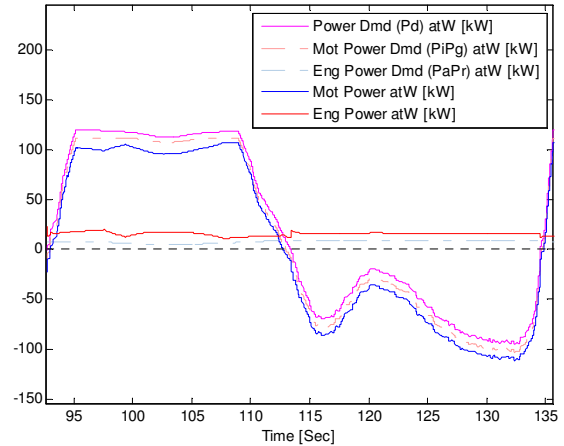


Figure 9: Power demand comparison for Hybrid vehicle with simple power split - full motor mode.

Hybrid vehicle with simple power split – motor limit mode

In this simulation run a simple power split strategy was utilized for motor power (Eq 16-19) for the Primary, Trails and Secondary drive cycles. The initial SOC, Electrical accessory loads and brakes were simulated same as in the last set. A SOC function was used to limit motor propulsion

power so that the final SOC is equal to initial SOC for fuel efficiency comparison for all these simulations. The results are summarized in Table 3. Figure 10 shows the effects of applying motor propulsion limits and it can be seen that due to these limits the engine needs to provide the remaining P_i+P_g for the propulsion i.e. positive component of the demanded power.

Sim	Model/Vehicle	Primary Roads	Trails	Secondary Roads
		Diff wrt actual (7711kg), baseline and eng only(%)	Diff wrt actual (7711kg), baseline and eng only(%)	Diff wrt actual (7711kg), baseline and eng only(%)
4	Hybrid veh with Simple power split- Motors Limited HEV with mot power limits, dynamic acc load offset	46.4% 45.2% 10.8%	39.3% 38.0% 14.6%	22.7% 27.0% 3.7%

Table 3: Simulation results for Hybrid vehicle with simple power split - motor limit mode.

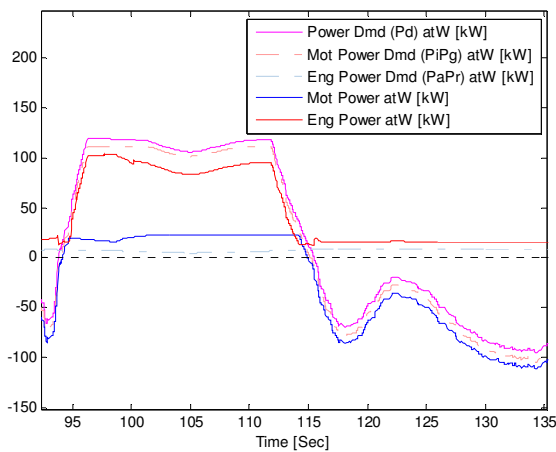


Figure 10: Power demand comparison for Hybrid vehicle with simple power split – motor limit mode.

Hybrid vehicle with efficiency based motor power split - motor limit mode

In this simulation run an efficiency-based algorithm was used for the motor power split between ISG and FMOT. The initial SOC, Electrical accessory loads and brakes were simulated same as in the last set and a similar SOC function was used to obtain final SOC close to the initial SOC. Table 1 summarizes the fuel consumption improvement over the actual and baseline vehicle simulation for the three drive cycles. Figure 11 graphically shows the Engine, ISG and FMOT power split based on the road loads and the

efficiency based algorithm. The switching of P_i+P_g power in order to maximize efficiency, between the FMOT and ISG can be seen.

Sim	Model/Vehicle	Primary Roads	Trails	Secondary Roads
		Diff wrt actual (7711kg), baseline and eng only(%)	Diff wrt actual (7711kg), baseline and eng only(%)	Diff wrt actual (7711kg), baseline and eng only(%)
5	Hybrid veh - Efficiency based mot power split HEV with mot limits and efficiency based power split and dynamic acc load offset	48.9% 47.8% 15.1%	44.5% 43.3% 21.9%	24.7% 28.9% 6.2%

Table 4: Simulation results for Hybrid vehicle with efficiency based motor power split - motor limit mode.

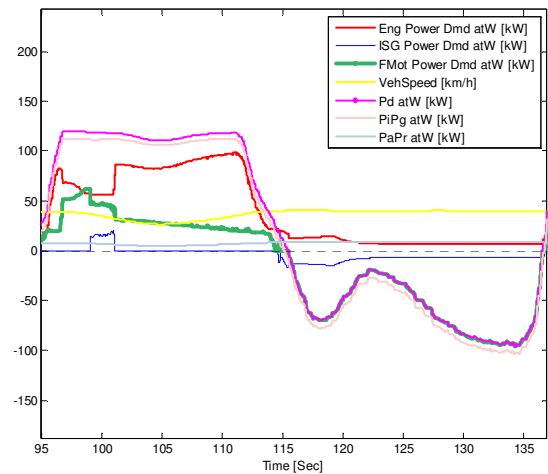


Figure 11: Power demand comparison for Hybrid vehicle with efficiency based motor power split – motor limit mode.

Following figures [12, 13 and 14] show an example of FMOT, ISG and Engine operating points and the % time during a drive cycle that they spend at these operating points. The objective of the algorithm was to operate FMOT, ISG and Engine as close as possible to the maximum efficiency regions.

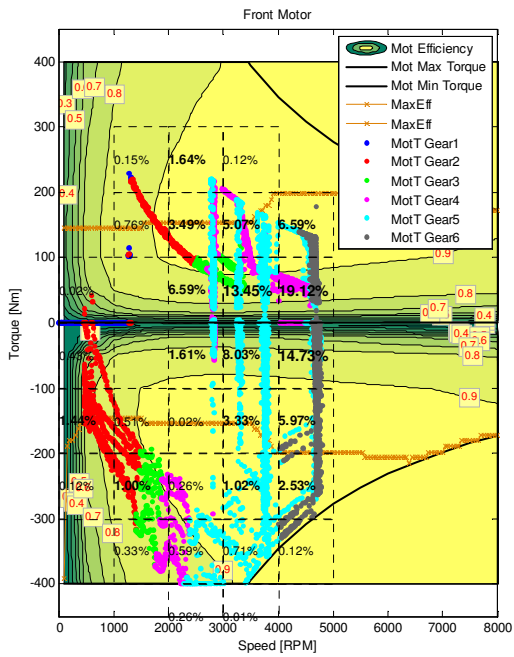


Figure 12: Front motor operation points

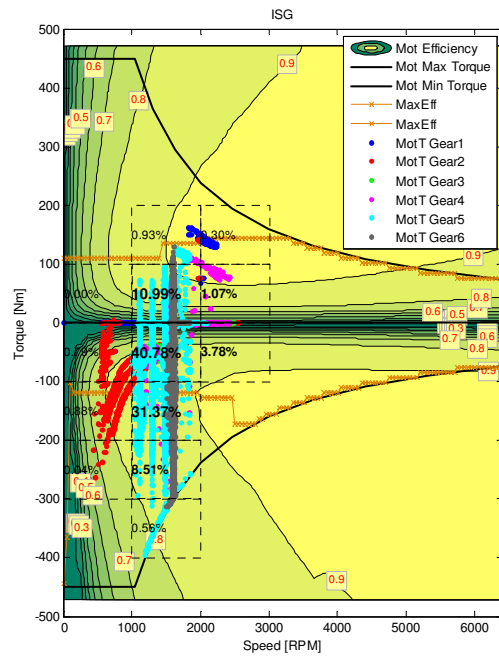


Figure 14: ISG operation points

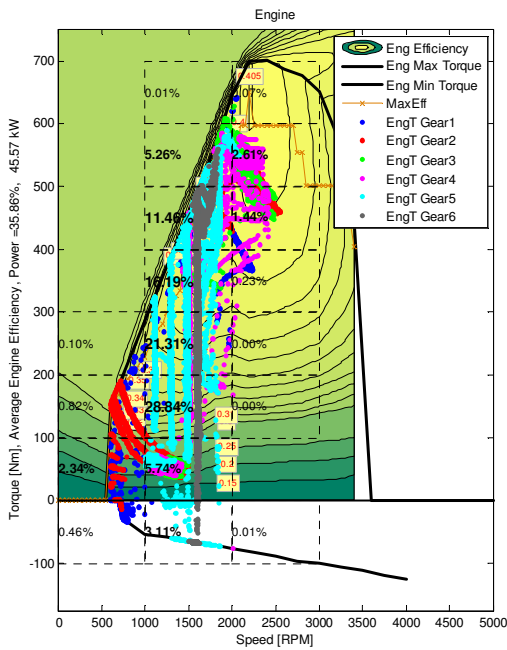


Figure 13: Engine operation points

CONCLUSIONS

This paper presents an efficient energy management strategy that includes a unique power split & energy distribution. The energy distribution is initially based on calculated vehicle road loads then on an efficiency-based optimization algorithm to further split the motor power between the front and the rear.

The results show an overall 41- 92 % improvement over the baseline vehicle simulation that includes a 7 - 28% improvement due to hybridization.

REFERENCES

- [1] J. B. Holtz, F. Uppal and P Naick, 2011, "Efficient Hybrid Propulsion System Development and Vehicle Integration", 2011 NDIA Ground Vehicle Systems Engineering and Technology Symposium, Modeling & Simulation, Testing and Validation (MSTV) Mini-Symposium, August 9-11 Dearborn, Michigan.
- [2] William F. Milliken and Douglas L. Milliken, Race Car Vehicle, Aug 1995, Society of Automotive Engineers Inc, ISBN-10: 1560915269, ISBN-13: 978-1560915263.
- [3] A Dowling, 2009, The Michigan Chemical Process Dynamics and Controls Open Text Book, May 2009, https://controls.engin.umich.edu/wiki/index.php/Electric_VehicleCruiseControl.
- [4] J. C. Lagarias, J. A. Reeds, M. H. Wright, and P. E. Wright, "Convergence Properties of the Nelder-Mead Simplex Method in Low Dimensions," *SIAM Journal of Optimization*, Vol. 9, Number 1, pp. 112–147, 1998.
- [5] G. R. Walsh, Methods of optimization, John Wiley and Sons, London, New. York, Sydney and Toronto, 1975. ISBN: 0471919225.